

Accepted Manuscript

Characterization of disinfection byproduct formation and associated changes to dissolved organic matter during solar photolysis of free available chlorine

Tessora R. Young, Wentao Li, Alan Guo, Gregory V. Korshin, Michael C. Dodd



PII: S0043-1354(18)30726-7

DOI: [10.1016/j.watres.2018.09.022](https://doi.org/10.1016/j.watres.2018.09.022)

Reference: WR 14072

To appear in: *Water Research*

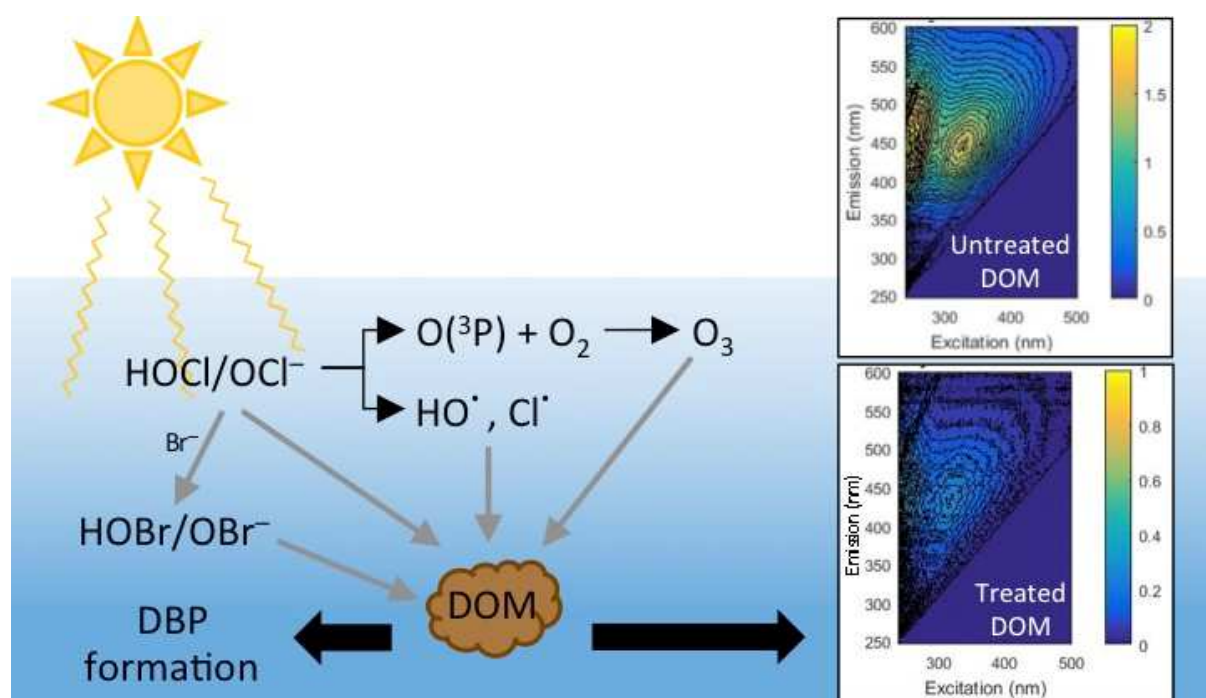
Received Date: 26 April 2018

Revised Date: 24 July 2018

Accepted Date: 5 September 2018

Please cite this article as: Young, T.R., Li, W., Guo, A., Korshin, G.V., Dodd, M.C., Characterization of disinfection byproduct formation and associated changes to dissolved organic matter during solar photolysis of free available chlorine, *Water Research* (2018), doi: <https://doi.org/10.1016/j.watres.2018.09.022>.

This is a PDF file of an unedited manuscript that has been accepted for publication. As a service to our customers we are providing this early version of the manuscript. The manuscript will undergo copyediting, typesetting, and review of the resulting proof before it is published in its final form. Please note that during the production process errors may be discovered which could affect the content, and all legal disclaimers that apply to the journal pertain.



Characterization of Disinfection Byproduct Formation and Associated Changes to Dissolved Organic Matter During Solar Photolysis of Free Available Chlorine

Tessor R. Young,[†] Wentao Li,[‡] Alan Guo,[†] Gregory V. Korshin,[†] Michael C. Dodd,^{†,*}

[†] Dept. of Civil and Environmental Engineering, University of Washington, Seattle, WA

[‡] State Key Laboratory of Pollution Control and Resources Reuse, School of the Environment,
Nanjing University, Nanjing, 210023, China

Author e-mail addresses: try4@uw.edu, liwentao@nju.edu.cn, ahg8@uw.edu, korshin@uw.edu,
doddm@uw.edu

*Corresponding author contact details:

305 More Hall, Box 352700; Seattle, WA 98195-2700
206-685-7583; fax: 206-543-1543; e-mail: doddm@uw.edu

Word Count: Overall: 8116 (Text: 6490, References: 1626)

Keywords: Chlorine, Solar irradiation, Ozone, Hydroxyl radical, Disinfection byproducts,
Dissolved organic matter

Abstract

Solar irradiation of chlorine-containing waters enhances inactivation of chlorine-resistant pathogens (e.g., *Cryptosporidium* oocysts), through in situ formation of ozone, hydroxyl radical, and other reactive species during photolysis of free available chlorine (FAC) at UVB-UVA wavelengths of solar light (290-400 nm). However, corresponding effects on regulated disinfection byproduct (DBP) formation and associated dissolved organic matter (DOM) properties remain unclear. In this work, when compared to dark chlorination, sunlight-driven FAC photolysis over a range of conditions was found to yield higher DBP levels, depletion of DOM chromophores and fluorophores, preferential removal of phenolic groups versus carboxylic acid groups, and degradation of larger humic substances to smaller molecular weight compounds. Control experiments showed that increased DBP levels were not due to direct DOM photolysis and subsequent dark reactions with FAC, but to co-exposure of DOM to FAC and reactive species (e.g., O_3 , HO^\bullet , Cl^\bullet , Cl_2^\bullet , ClO^\bullet) generated by FAC photolysis. Because solar chlorine photolysis can enable inactivation of chlorine-resistant pathogens at far lower CT_{FAC} values than chlorination alone, the increases in DBP formation inherent to this approach can likely be offset to some extent by the ability to operate at significantly decreased CT_{FAC} . Nonetheless, these findings demonstrate that applications of solar chlorine photolysis will require careful attention to potential impacts on DBP formation.

1. Introduction

Free available chlorine (FAC) is the most commonly applied chemical disinfectant worldwide (WHO 2017). However, some important waterborne microorganisms are chlorine-resistant and persist after disinfection with FAC. For instance, highly chlorine-resistant oocysts of the protozoan parasites *Cryptosporidium hominis* and *Cryptosporidium parvum* are a frequent cause of waterborne illness in the United States and worldwide (Medema 2009, Painter et al. 2015). Ultraviolet (UV) irradiation and ozonation are both recognized alternative disinfection strategies that can be applied to achieve inactivation of protozoan (oo)cysts and other chlorine-resistant microorganisms; nevertheless, monetary and energy expenses may prevent their use in small-scale drinking water treatment applications (Cho et al. 2006, EPA 2005).

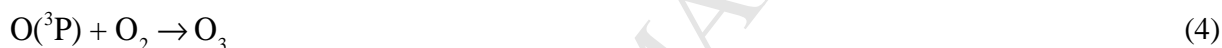
Exposing chlorinated water to sunlight has been reported to dramatically enhance inactivation of chlorine-resistant *Bacillus subtilis* endospores and highly-chlorine resistant *Cryptosporidium* oocysts when compared to chlorination alone (Forsyth et al. 2013, Zhou et al. 2014). Photolysis of free available chlorine (FAC) by solar wavelengths of UV light (i.e., UVB and UVA wavelengths from 290-400 nm, which overlap with the absorption spectra for HOCl and OCl⁻; Figure S2a) produces hydroxyl radical (HO[•]), chlorine atom (Cl[•]), and atomic oxygen (O³(P)); the latter of which reacts with dissolved oxygen (O₂) to form ozone (O₃) (Table 1, Equations 1-4) (Buxton and Subhani 1972, Forsyth et al. 2013, Nowell and Hoigne 1992a, b, Oliver and Carey 1977, Zhou et al. 2014). O₃ and HO[•] in particular are strong oxidants that can enhance disinfection during chlorination by damaging or penetrating protective spore and cyst coats (Cho and Yoon 2007, 2008, Forsyth et al. 2013, Zhou et al. 2014). Considering the low cost and widespread availability of FAC and sunlight, solar FAC photolysis could provide a uniquely effective option for enhancing disinfection in decentralized and point-of-use treatment,

especially in low-resource settings – for example, by combining chlorination with conventional solar disinfection (SODIS) (McGuigan et al. 2012).

Table 1. Summary of chlorine photolysis reactions and quantum yields

		$\Phi(254\text{ nm})$	$\Phi(313\text{ nm})$	$\Phi(365\text{ nm})$
$\text{HOCl} + h\nu \rightarrow \text{HO}^\bullet + \text{Cl}^\bullet$	(1a)	0.46-1.4 ^{a-c}	1 ^{d*}	N/A
$\text{OCl}^- + h\nu \rightarrow \text{O}^\bullet + \text{Cl}^\bullet$	(1b)	0.278 ^c	0.127 ^c	0.08 ^c
$\text{OCl}^- + h\nu \rightarrow \text{O}({}^3\text{P}) + \text{Cl}^-$	(2)	0.074 ^c	0.075 ^e	0.28 ^e

^a(Watts et al 2007), ^b(Jin et al 2011), ^c(Wang et al 2012), ^{*}at approximately 310 nm ^d(Molina et al 1980), ^e(Buxton and Subhani 1972), N/A = not available



While the potential of solar FAC photolysis for mitigating acute health risks (by enabling inactivation of chlorine-susceptible *and* chlorine-resistant pathogens) has been demonstrated (Forsyth et al. 2013, Zhou et al. 2014), its possible long-term health implications (e.g., effects on disinfection byproduct formation) must also be explored before recommending its use.

FAC and the various oxidants generated during FAC photolysis also react with inorganic and organic water constituents, such as bromide and dissolved organic matter (DOM), that can serve as disinfection byproduct (DBP) precursors. An abundance of investigations have evaluated DBP formation in DOM-containing waters during UVC-driven (200-280 nm) FAC photolysis – in which HOCl and OCl⁻ undergo primarily homolytic cleavage to form HO[•] and Cl[•] (Eqs. 1a,b). However, conflicting results have been reported regarding whether FAC+UVC treatment leads to *increased* DBP formation (e.g., due to precursor formation via hydroxylation and aromatic ring opening by hydroxyl radical or other radical species (Pisarenko et al. 2013, Wang et al. 2015,

Xiang et al. 2016)) or decreased DBP formation due to precursor degradation (Li et al. 2016, Wang et al. 2017), when compared to chlorination alone (Liu et al. 2012, Remucal and Manley 2016, Yang et al. 2016).

Comparatively little information is available regarding the potential impacts of sunlight-driven FAC photolysis on DBP formation (Nowell and Hoigne 1992b, Oliver and Carey 1977, Pisarenko et al. 2013, Simard et al. 2013). In comparison to UVC-driven FAC photolysis, solar FAC photolysis ($\lambda > 290$ nm) proceeds to a much greater extent through OCl^- heterolysis (particularly at pH above the pK_a of HOCl ; Eq. 3) – yielding ground-state atomic oxygen (Eq. 2), in addition to O_3 under oxic conditions (Eq. 4) (Buxton and Subhani 1972). Previous work investigating sequential exposure of DOM to O_3 and chlorine has shown that *high* O_3 doses can *decrease* DBP formation by degrading DBP precursors, whereas *low* O_3 doses can actually result in *increased* DBP formation, especially under conditions favoring HO^\bullet formation (De Vera et al. 2015, Mao et al. 2014, Riley and Mancy 1978). The impacts of simultaneous DOM exposure to FAC, O_3 , and HO^\bullet or other radicals during solar FAC photolysis are less clear, and to the authors' knowledge, a comprehensive evaluation of this reaction chemistry has yet to be undertaken. Several groups have noted decreases in total organic halogens (TOX) within reclaimed water (Lv et al. 2017), and degradation of naphthenic acids within oil sand process water (Shu et al. 2014) after sunlight-driven FAC photolysis. Others have reported increasing formation of organochlorine, trihalomethanes (THMs), and haloacetic acid (HAAs), coupled with significant degradation of chromophores and fluorophores, during treatment of organic precursors with FAC and artificial UVA light sources ($\lambda_{\text{peak}} \sim 350\text{--}365$ nm) when compared to dark chlorination (Oliver and Carey 1977, Pisarenko et al. 2013). However, there is limited information on formation of specific classes of DBPs during broadband simulated or natural

solar irradiation of chlorinated water, or the corresponding impacts on DOM and DBP precursors during the application of this process for drinking water treatment.

Furthermore, available data on DBP formation during UV or sunlight-driven FAC photolysis has generally been reported only for conditions in which water samples were subjected to either (i) varying initial FAC concentrations for fixed irradiation times, or (ii) fixed initial FAC concentrations for variable irradiation times, without accounting for variations in FAC concentration and consequent effects on cumulative FAC exposure ($CT_{\text{FAC}} = \int_0^t [\text{FAC}] dt$) during irradiated and dark treatment. This is an important limitation, as DBP formation is dependent on both FAC concentration *and* reaction time and is expected to be strongly influenced by variations in FAC concentrations during irradiation. Without the availability of measurements of CT_{FAC} (which normalizes for variations in FAC concentration *and* reaction time) from the prior studies, it remains unclear how CT_{FAC} -specific DBP formation potentials are affected by sunlight-driven FAC photolysis, in turn hindering direct comparison of DBP formation under dark and light conditions.

The principal objectives of this work were to (a) quantify formation of regulated organic DBPs (THMs and HAAs) during sunlight-driven FAC photolysis, and (b) correlate DBP formation with characteristic changes to DOM during dark chlorination, solar irradiation, and sunlight-driven FAC photolysis. DBP formation was investigated under a variety of conditions (e.g., varying pH, temperature, bromide concentration, or O_2 concentration; w/ and w/o added oxidant scavengers; etc.). The effects of variations in FAC exposure were normalized to CT_{FAC} to enable comparison of CT_{FAC} -specific DBP formation under the range of conditions investigated. Corresponding changes in DOM character were investigated by monitoring changes in DOC, fluorescence excitation-emission matrices (EEMs), UV absorbance (UV_{254} specifically),

differential absorbance spectra, and size-exclusion chromatographs of the DOM present in treated solutions. An overarching objective of this work was to utilize these analyses to provide an improved understanding of how DOM modifications resulting from solar irradiation in the presence of FAC influence DBP yields, and how this knowledge may be applied to mitigate such impacts during the use of this approach to enhance inactivation of chlorine-resistant microorganisms for drinking water treatment applications.

2. Materials and Methods

2.1. Materials. The reverse osmosis isolate of Suwannee River NOM (SRNOM) was obtained from the International Humic Substance Society (batch number 2R101N). All other chemicals, unless specified otherwise, were obtained from Sigma Aldrich and were of at least reagent-grade purity. All aqueous stock solutions were prepared in Milli-Q ultrapure water with resistivity ≥ 18.2 M Ω cm. Detailed descriptions of chemical and natural water sample sources and stock solution preparation are provided in the Supplementary Material, Text S1.

2.2. Chlorine and Simulated Sunlight Treatment Procedures. Experiments were undertaken in duplicate using buffered reagent water solutions (10mM phosphate unless otherwise specified, at pH 8.0 or 6.0) or natural water samples (details and characterization in Text S1 and Table S1) according to four treatment protocols: (i) dark chlorination (FAC only), (ii) simulated solar irradiation without FAC followed by a dark FAC period (Light only/FAC only), (iii) simulated solar irradiation of FAC-containing water for varying times followed by dark FAC treatment (FAC+light/FAC only), and (iv) simulated solar irradiation of FAC-containing water for varying times *without* subsequent dark FAC treatment (FAC+light). All simulated solar irradiations were conducted within an Atlas Material Testing Solutions

SUNTEST XLS+ solar simulator equipped with a 1700-W, O₃-free, Xe arc lamp with daylight filter (cutoff below 290 nm) and infrared radiation filter. Irradiations of samples in quartz reactor tubes were undertaken at either 10 or 25 °C (maintained by means of a recirculating water bath). Detailed descriptions of reactor configurations and experimental procedures (including rationale for selection of FAC concentrations, irradiation times, and CT_{FAC} values utilized in experiments) are provided in Text S2-S3 and Figure S1.

Chemical actinometry experiments, using *para*-nitroanisole and pyridine (Dulin and Mill 1981, Laszakovits et al. 2017), were performed in quartz reactor tubes alongside sample irradiation experiments (Text S4). Periodic spectral irradiance measurements were obtained using a USB2000+ XR spectroradiometer (Ocean Optics) equipped with a 200 $\mu\text{m} \times 2\text{ m}$ optical fiber and CC-3-UV-S cosine corrector (see Figure S2b for representative spectral irradiance curves).

2.3. Natural Sunlight Experiments. Experiments using natural sunlight followed the same general procedures as simulated sunlight experiments, except that samples were exposed to sunlight on the roof of More Hall at the University of Washington. Incident fluence data is included in Figure S3, and a representative spectral irradiance curve is included in Figure S2b.

2.4. Ozone Experiments. One-hundred mL of 2 mg/L SRNOM solutions (pH 8, 0.5-mM phosphate buffer, w/ or w/o 50-mM *tert*-butanol (*t*-BuOH)) were dosed in duplicate with aqueous O₃ at concentrations ranging from 0.25-1 g O₃/g DOC, and allowed to react to complete O₃ consumption prior to analyses. See Text S1 for details on O₃ stock solution preparation.

2.5. Analytical Methods. **2.5.1. DBP Extraction and Analysis.** Twenty mL volumes of Na₂S₂O₃-quenched sample were acidified to pH < 2 with 98% purity H₂SO₄. After increasing the aqueous ionic strength with sodium sulfate, THMs and protonated HAAs were then extracted

into 4 mL of MTBE amended with internal standards (100 µg/L 1,2,3-trichloropropane and 2,3-dibromopropanoic acid) via vigorous mixing. Subsequently, the supernatant MTBE layer containing THMs and HAAs was separated from the underlying aqueous phase via pipetting and transferred into a separate conical-bottom borosilicate glass vial. HAAs were esterified by adding 1 mL of acidified methanol (10% volume H₂SO₄) to 3 mL of the MTBE extract and heating at 50 °C for 2 hours. After esterification, excess acid was neutralized with 4 mL of saturated aqueous sodium bicarbonate, and 1mL of neutralized MTBE supernatant was transferred to autosampler vials for analysis (Munch 1995). THMs and HAAs were analyzed using a Shimadzu GC-2010 with HP-1MS U column and electron-capture detector.

2.5.2. Absorbance and Fluorescence Measurements. Samples quenched with As(III), a fast-reacting (Dodd et al. 2006) inorganic FAC quencher with negligible UV absorbance at $\lambda > 220$ nm, were analyzed by UV and fluorescence spectrophotometry. UV-Vis absorbance spectra were recorded from 224 - 800 nm and fluorescence EEMs recorded over an excitation range of 240 - 600 nm and an emission range of 245.2 - 826.6 nm. Both measurements were collected within a 1 cm quartz cuvette using a HORIBA Aqualog 800-C spectrofluorometer (details in Text S5).

2.5.3. UV-Vis Differential Absorbance Spectrophotometry (DAS). As per established methods (Dryer et al. 2008, Gao and Korshin 2013), after completion of experiments 40 mL of 0.5-mM phosphate-buffered samples were quenched with Na₂S₂O₃ in two-fold excess of FAC and acidified to pH ~ 2.9 by addition of 1 M HClO₄. Samples were gradually titrated with NaOH (1 M) at 0.5-unit pH intervals, and absorbance spectra recorded in a 5-cm quartz cell within a Shimadzu UV2700 spectrophotometer (details in Text S6). DAS spectra were obtained using Equation 5, where $A_{pH(\lambda)}$ is the absorbance (measured between 200 to 600 nm) at varied pH, $A_{pH_Ref(\lambda)}$ is the reference absorbance acquired at pH ~2.9, and l_{cell} is the quartz cell path length.

$$\Delta A_{\text{pH}(\lambda)} = \frac{A_{\text{pH}(\lambda)} - A_{\text{pH_Ref}(\lambda)}}{l_{\text{cell}} \times \text{DOC}}; \text{ units of } L / (\text{mg} \cdot \text{cm}) \quad (5)$$

2.5.4. *Size Exclusion Chromatography (SEC)*. As(III)-quenched samples were also analyzed by SEC with inline UV, fluorescence, and DOC detection. One-hundred μL injection volumes of each sample were resolved by size/molecular weight using a Tosoh Toyopearl HW-50S (250 mm x 20 mm, 3 μm) column installed on a Dionex UltiMate3000 HPLC operated at 1 mL/min with a mobile phase of 13.8 mM phosphate buffer at pH 6.8 and 0.1 M ionic strength (with ionic strength adjustment using NaClO_4). The HPLC-SEC system was equipped with a UV diode array detector, fluorescence detector, and GE Sievers 900 Series Turbo online organic carbon detector equipped with an inline inorganic carbon remover (additional details in Text S7).

3. Results and Discussion

3.1. Disinfection Byproduct Formation. *3.1.1. General effects of FAC photolysis on DBP formation.* Figure 1 compares concentrations of HAA5 (mono-, di-, and trichloroacetic acids, and mono- and dibromoacetic acids) and TTHM (chloroform, bromodichloromethane, dibromochloromethane, and bromoform) formed during exposure of phosphate buffered solutions containing 2 mg/L of SRNOM and 8 mg/L as Cl_2 of FAC to varying irradiation times (0, 15, 30, and 45 minutes of simulated sunlight, equal to 0, 6.2, 12.4, and 18.6 J/cm^2 fluence), coupled with post-irradiation dark FAC exposure up to a cumulative CT_{FAC} of 400 $(\text{mg}/\text{L}) \times \text{min}$. As shown in Figure 1, there is a clear increase in DBP formation during FAC+light/FAC only treatment when compared to FAC only treatment for all conditions. Elevated temperature resulted in further increases in DBP formation at each condition (Figure 1), which appears to be due primarily to increased rates of dark DOM chlorination (Text S8). Direct solar irradiation

(and hence direct DOM photolysis) did not appear to be an important contributor to DBP formation. Even at the highest fluence investigated (18.6 J/cm^2) HAA5 and TTHM yields after light only/FAC only treatment were similar to those measured following FAC only treatment (Table S3). Similar trends were also observed when using natural sunlight to photolyze FAC (Figure S3).

As discussed in more detail below, the increases in THM and HAA formation during solar FAC photolysis may result from DOM modifications predisposing certain DBP precursor constituents to increased halogenation during co-exposure to FAC, O_3 , and various reactive oxygen or halogen species (ROS or RHS) generated by FAC photolysis. While prior work has shown that pre-ozonation of DOM at $\sim 0.4\text{--}1 \text{ mg O}_3/\text{mg C}$ and circumneutral pH can *decrease* THM formation during chlorination (Gallard and von Gunten 2002, Hua and Reckhow 2013), pre-oxidative treatment at lower O_3 exposures and/or elevated HO^\bullet exposures (e.g., during O_3 treatment at high pH or AOPs such as $\text{UV/H}_2\text{O}_2$) – similar to the conditions of solar FAC photolysis – has actually been shown to *increase* THM formation during chlorination (De Vera et al. 2015, Dotson et al. 2010, Mao et al. 2014, Riley and Mancy 1978). This is thought to be due to degradation of higher molecular weight humic-like substances to smaller, chlorine-reactive alcohol or ketone-containing aromatic or aliphatic groups (De Vera et al. 2015, Dotson et al. 2010, Mao et al. 2014, Riley and Mancy 1978).

In additional experiments, bromide was added to reaction solutions at concentrations of 40 or $200 \mu\text{g/L}$, in order to evaluate formation of brominated DBPs under conditions representative of relatively pristine or human-influenced surface waters (Flury and Papritz 1993, Soltermann et al. 2016). Addition of bromide led to suppression of HAA5 and TTHM yields during both FAC only and FAC+light/FAC only treatments (Figure 1). In contrast, HAA9 – which includes

additional mixed Cl⁻ and Br⁻-containing HAAs not captured by HAA5 – remained relatively constant at elevated bromide levels during FAC only treatment (Figure S6a) (consistent with prior observations (Chellam and Krasner 2001, Cowman and Singer 1996)), and increased at elevated bromide levels during FAC+light/FAC only treatment (Figure S6a). In addition, bromine substitution factor (BSF) – a measure of the fraction of total DBP halogen content attributable to bromine (Text S9) – increased for TTHM *and* HAA9 during FAC only and FAC+light/FAC only treatments at elevated bromide levels, with a relatively larger increase in BSF observed during FAC+light/FAC only treatment (Figure S6). This suggests increased bromination during FAC+light/FAC only treatment compared to FAC only treatment – potentially due to modifications to DOM during FAC photolysis (leading to greater susceptibility of DBP precursors to bromination), or direct bromination of DBP precursors by photochemically-generated reactive bromine species such as Br[•] or BrCl^{•+}.

pH effects on FAC speciation or photolysis pathway (Eq. 1-4) did not seem to have a clear influence on HAA formation, as variation of pH did not have a strong effect on HAA5 (Figure 1a,b) or HAA9 (Figure S6a) yields during either FAC only or FAC+light/FAC only treatment. Prior investigations have also reported variability in the pH-dependence of overall HAA formation during dark chlorination and FAC photolysis processes, though trihaloacetic acid formation generally appears to correlate inversely with pH during dark chlorination (Korshin et al. 2002, Liang and Singer 2003, Remucal and Manley 2016, Wang et al. 2015). In contrast, TTHM yields in the present work increased with increasing pH for both FAC only and FAC+light/FAC only treatment (Figure 1c,d), consistent with prior observations (Gallard and von Gunten 2002, Pisarenko et al. 2013, Rook 1977). In addition to an increased importance of OH⁻ in the haloform reaction at higher pH, increased TTHM yields during FAC+light/FAC only

treatment may be in part related to solar FAC photolysis kinetics, as the rate of FAC photolysis increases with pH at wavelengths above 260 nm due to increased UV absorbance by FAC with the shift in speciation from HOCl to OCl⁻ (Eqs. 1-4, Figure S2a) (Nowell and Hoigne 1992a, b).

3.1.2. Effects of dissolved O₂ removal and radical scavenger addition. In order to evaluate the relative importance of O₃ and radical species in driving DBP formation during FAC+light/FAC only treatment, concentrations of O₂ were varied from ~0 to 1.6 mmol/L and the radical scavengers *t*-BuOH or carbonate (as NaHCO₃) were added separately at concentrations of 50 mM to selected reaction solutions (Figure 2).

Initially anoxic conditions are expected to limit formation of O₃ by preventing the reaction of photochemically-generated O(³P) with O₂, whereas saturation with O₂ is anticipated to increase O₃ formation relative to ambient conditions (as per Eq. 4). Addition of 50 mM concentrations of *t*-BuOH or carbonate is anticipated to lead to 97% or 41% scavenging of HO[•], 95% or 88% scavenging of Cl[•], and 53% or 4% scavenging of O(³P) under the experimental conditions investigated here (Text S10 and Table S4).

The absence of O₂ did not appear to lead to significant differences in HAA5 yields, whereas O₂ saturation led to moderate decreases in HAA5 yields, indicating that O₃ may contribute to destruction of HAA precursors during FAC photolysis (Figure 2a). Figure 2b shows that the absence of O₂ resulted in a small increase in TTHM yields during FAC+light/FAC only treatment, possibly due to decreased destruction of THM precursors (e.g., dihydroxybenzenes) by O₃ (Gallard and von Gunten 2002, Hua and Reckhow 2013). O₂ saturation had no clear effect on THM yields during FAC+light/FAC only treatment.

Addition of *t*-BuOH and carbonate each appeared to result in modest decreases in HAA5 yields (Figure 2a) during FAC+light/FAC only treatment, due in large part to decreases in di-

and trichloroacetic acid formation (Figure 2a and Figure S6a). This indicates that radical reactions with DOM may contribute to HAA precursor formation. Carbonate and *t*-BuOH addition did not have a clear effect on TTHM yields during FAC+light/FAC only treatment (Figure 2b). Overall, variations in dissolved O₂ concentrations and addition of radical scavengers resulted in at most modest changes to organic DBP formation, making it difficult to distinguish direct effects of O₃ and radical species (e.g., HO[•], Cl[•], Cl₂^{•-}, ClO[•], O(³P)) on DBP precursors.

3.1.3. Importance of photochemical versus dark reactions in driving DBP formation. Figure 3 compares DBP formation versus CT_{FAC} during FAC only treatment and FAC+light treatment (labeled 15, 30, and 45 minutes) *without* and *with* post-irradiation dark FAC treatment. Compared to FAC only treatment, FAC+light treatment resulted in substantially greater yields of THM and HAA5 at a given CT_{FAC} value, confirming that yields of DBPs are elevated *during* sunlight-driven FAC photolysis. Figure 3 also highlights the change in DBP formation resulting from continued FAC only treatment *after* sunlight-driven FAC photolysis by comparing the results for FAC+light treatment (open symbols) with those for FAC+light/FAC only treatment (half-filled symbols), with the same irradiation times used in each case. It appears that the CT_{FAC}-normalized rate of HAA5 formation during dark chlorination (Figure 3, solid lines) increases modestly after FAC+light treatment (regression slopes increase by factors of 2 and 3 for pH 8 and 6, respectively), whereas the rate of TTHM formation during dark chlorination (Figure 3, dashed lines) is similar after FAC+light and FAC only pretreatment when normalized by CT_{FAC}. Taken together, these data indicate that most (if not all) of the *relative increases* in DBP yields observed during FAC+light/FAC only experiments are due to DBP formation during FAC photolysis, rather than to post-irradiation reactions in the dark. This in turn suggests that increases in DBP formation during sunlight-driven FAC photolysis are driven primarily by

halogenation reactions *during* irradiation (consistent with (Oliver and Carey 1977)), though it is unclear if this is due to (i) direct halogenation of DOM by RHS (e.g., Cl^\bullet , Br^\bullet , BrCl^\bullet , Cl_2^\bullet , ClO^\bullet), (ii) oxidative modifications to DOM resulting in generation of precursor moieties with higher susceptibility toward halogenation by FAC (or RHS), or (iii) a combination of both.

3.1.4. DBP formation during treatment of natural waters. Figure 4 shows HAA5 and TTHM yields in two natural freshwaters – Lake Washington and a local reservoir; with and without addition of 200 $\mu\text{g/L}$ of bromide – subjected to (i) FAC only, (ii) Light only/FAC only, and (iii) FAC+light/FAC only treatment. FAC only and Light only/FAC only treatment (at fluences up to 18.6 J/cm^2) resulted in similar DBP yields, indicating that direct photolysis of the DOM does not impact DBP formation during chlorination. HAA5 concentrations associated with Lake Washington remained well below the EPA MCL of 60 $\mu\text{g/L}$ and were not detected within the local reservoir water. TTHM formation was compliant with the EPA MCL of 80 $\mu\text{g/L}$ at natural bromide concentrations for each water, though at higher bromide concentrations, formation of bromodichloromethane and dibromochloromethane increased during solar FAC photolysis, and TTHM levels exceeded the MCL. These results indicate that sunlight-driven FAC photolysis can likely be applied for disinfection of natural waters with relatively low DOM and bromide concentrations, though further work is needed to evaluate its applicability over a wider range of water qualities.

3.2. Analyses of Changes to Dissolved Organic Matter. **3.2.1. UV-Vis Absorbance and Fluorescence.** The results summarized in Figure 5a, Figure S7a, and Table S5 show that SRNOM after FAC+light treatment has substantially lower 254 nm UV absorbance than after FAC only treatment. Addition of *t*-BuOH results in preservation of chromophores during solar FAC photolysis (31% and 51% losses in 254 nm absorbance with and without *t*-BuOH

respectively, after 45 minutes of FAC+light). Anoxic conditions also result in preservation of chromophores during solar FAC photolysis treatment, but to a lesser extent than *t*-BuOH addition (40% loss after 45 minutes of FAC+light); indicating that radical species and O_3 contribute to decreases in absorbance and destruction of associated aromatic compounds.

Untreated SRNOM has characteristic fluorescence features, including two peaks located near 250 nm_{Ex} / 450 nm_{Em} and 330 nm_{Ex} / 450 nm_{Em}, that are typically associated with terrestrial humic constituents (Hua et al. 2010, Ishii and Boyer 2012). DOM with high fluorescence intensity in these regions has been positively correlated to THM formation during chlorination (Hua et al. 2010, Li et al. 2016). Figure S8 depicts the change to fluorescence EEMs after FAC only, Light only, Light only/FAC only, FAC+light, and FAC+light/FAC only treatment. FAC+light and FAC+light/FAC only treatments resulted in significantly greater losses in the fluorescence signals associated with humic constituents when compared to FAC only, Light only, or Light only/FAC only treatments (Figure 5a, S7a). Previous research also observed greater fluorophore destruction during FAC-UVA treatment when compared to FAC-UVC AOP treatment (Pisarenko et al. 2013) and FAC-only treatment (Shu et al. 2014).

Introducing *t*-BuOH as a radical scavenger during solar chlorine photolysis significantly inhibited degradation of humic-like fluorophores, to an extent greater than observed by limiting O_3 formation under anoxic conditions (Figure 5a, S7a and Table S5). These trends indicate that photochemically-generated HO^\bullet , Cl^\bullet , or other ROS/RHS, and – to a lesser degree – O_3 , all play important roles in the degradation of fluorophores during FAC+light treatment.

3.2.2. UV-Vis Differential Absorbance Spectra (DAS). The pH titration DAS analysis method provides an in situ approach to quantifying behavior of ionizable chromophores, which reflects contributions of carboxylic and phenolic functional groups in DOM (Dryer et al. 2008, Gao and

Korshin 2013). A monotonic increase in UV absorbance (240-450 nm) of DOM is typically observed with increasing pH, which is primarily associated with deprotonation of aromatic DOM chromophores (Korshin et al. 1997). From the DAS results of raw SRNOM (Figure 6a) there are two prominent feature bands: a narrow band centered at ~280 nm (DA280) associated with carboxylic acid groups, and a broad band centered at ~340 nm (DA340) associated with phenolic groups (Dryer et al. 2008, Gao and Korshin 2013).

FAC only treatment of SRNOM-containing solutions at pH 8 and 6 resulted in moderate decreases in sample absorbance (Figure 6b, S9a,b), indicating that FAC reacted directly with chromophores within the DOM. The DA340/DA280 ratio for samples subjected to FAC only treatment at pH 8 and 6 did not change during titration from pH 6 to 10, indicating suppression of the phenol deprotonation feature compared to the untreated sample (Figure S9a,b). Light only treatment had no significant impact on DAS spectra (Figure S9a,b).

Exposing SRNOM-containing solutions to FAC+light treatment using natural (FAC+light_{NS}) or simulated sunlight (FAC+light_{SS}) at pH 6 and 8 resulted in substantially greater bleaching of UV absorbance compared to FAC only treatment, and particularly enhanced removal at 340 nm, indicating preferential modification of phenolic groups (Figures 6c, S9a,b). FAC+light treatment at pH 8 resulted in a lower average DA340/DA280 ratio than at pH 6, likely due to increased deprotonation of phenolic groups to more reactive phenolate forms and higher FAC photolysis rates at pH 8 (Figure S9a,b). The addition of bromide was found to have no significant effect on changes to the DA340/DA280 ratio before or after treatment (Figure S9b,c).

Changes in DAS spectra observed during FAC+light treatment at pH 8 were similar to those observed during treatment of samples with increasing O₃ doses (O₃/DOC > 0.75) (Figure 6c,f), where addition of *t*-BuOH had little effect on DAS changes during direct O₃ treatment (Figure

S9e). This is consistent with the proposed role of O_3 in contributing to direct degradation of phenolic groups in DOM during FAC+light treatment. However, purging O_2 from solution to limit the formation of O_3 during FAC+light treatment at pH 8 did not have a significant effect on DA340/DA280 ratios in comparison to FAC+ light_{ss} treatment at ambient O_2 levels (Figures 6d and S9d), suggesting either that O_3 plays a significantly less important role in driving phenol degradation compared to $O(^3P)$, HO^\bullet , Cl^\bullet , and other radical species, or that increased degradation of phenols by $O(^3P)$ (which would be elevated in the absence of O_2 , as per Eq. 4) compensates for the absence of O_3 . Adding *t*-BuOH as a radical scavenger limited decreases in DA340/DA280 ratios during FAC+light treatment to a moderate extent (Figure 6e and S9d), indicating some preservation of phenol groups due to suppression of ROS, RHS, and/or O_3 (via scavenging of $O(^3P)$) (Zhou et al. 2014).

3.2.3. Size Exclusion Chromatography with UV-fluorescence-DOC detection (SEC-UV-FLD-DOC). Size exclusion chromatography enables fractionation of DOM by size and/or molecular weight (MW), resulting in discrimination of two major peaks in the SRNOM comprising (1) a larger peak (Peak 1 here) assigned to higher MW humic substances and (2) a second, smaller peak (Peak 2 here) generally assigned to lower MW acidic compounds (Her et al. 2003, Huber et al. 2011) (see Figure S10 for example chromatograms). Figures 5b-d and S7b-d summarize results from chromatographic analyses of treated samples, including normalized total chromatogram area $((\text{Peak 1} + \text{Peak 2})_{\text{area}}/(\text{Peak 1} + \text{Peak 2})_{\text{area, untreated}})$ and average DOM MW estimates – each obtained using UV, fluorescence, and DOC detection (see Text S7 for analytical details and MW calculations and Figure S11 for plots of fractional peak areas).

FAC only treatment generally resulted in a decrease of <20% for UV chromatogram areas and 5-10% for total DOC areas, while a slight (~5%) increase in total fluorescence was visible –

an effect associated with halogenation of DOM (Korshin et al. 1999). Increasing periods of irradiation during FAC+light treatment resulted in decreases in overall MW as measured by UV and DOC detection, as well as 40-60% decreases in total UV chromatogram areas and up to 25% decreases in DOC chromatogram areas (Figures 5b,c, S7b-d). By comparison, fluorescence peak area decreased 20-80% with minimal changes to overall MW as measured by fluorescence (Figures 5d, S7d). These observations for FAC+light treatment are likely attributable to degradation of higher MW humic substances comprising Peak 1 to lower MW byproducts comprising Peak 2 (with little corresponding mineralization of DOC to CO₂), coupled with degradation of chromophores associated primarily with higher MW humic substances, and degradation of fluorophores associated with both higher and lower MW organics. Low MW byproducts that contribute to Peak 2 in DOC chromatograms after treatment appear to have a modest UV signal and very little fluorescence character (Figure S10).

Changes observable by DOC and UV detection were similar for each treatment at pH 8 and 6 (Figures 5b,c, S7b,c). Similar to bulk sample fluorescence and UV absorbance measurements, addition of *t*-BuOH resulted in preservation of chromophores and fluorophores and appeared to hinder degradation of larger MW compounds to lower MW compounds. This implies that HO[•], Cl[•], and other RHS species likely play an important role in breaking down aromatic molecules contained within larger DOM size fractions, though it should be noted that *t*-BuOH also scavenges O(³P) to a limited extent (Zhou et al. 2014), so some of the decreases in chromophore and fluorophore destruction may also have been due to blockage of reactions between O(³P) or O₃ and DOM. Suppressing O₃ formation by deoxygenation of reaction solutions prior to FAC+light treatment also resulted in decreased destruction of chromophores and fluorophores, but not to the same extent as *t*-BuOH addition. This suggests that O₃ may target a subset of

primarily electron-rich aromatic functional groups such as phenols and activated aromatic rings, whereas HO^\bullet , Cl^\bullet , and other radical species may less selectively attack a larger pool of aromatic components within the DOM.

3.3. Linkages between observed DOM modifications and increased DBP formation during sunlight-driven FAC photolysis. Decreases in fluorescence and UV absorbance of SRNOM exhibited clear correlations with THM and HAA9 yields during FAC+light treatment (Figure S12), whereas correlations for HAA5 yields were weaker (likely due to the smaller group of HAAs encompassed by HAA5 relative to HAA9). There were no clear trends between DBP formation and fluorescence or absorbance changes during FAC only treatment, providing additional evidence that modifications of DOM by ROS, RHS, and/or O_3 produced during FAC photolysis are associated with the observed increases THM and HAA yields.

The findings discussed to this point suggest that O_3 generated during solar FAC photolysis contributes to preferential elimination of SRNOM's humic-like fluorescence properties, which are likely attributable in part to activated/electron-rich aromatic rings (e.g., phenolic groups) (Cory and McKnight 2005, Sharpless and Blough 2014). Similarities in DA340/DA280 losses during FAC+light treatment and O_3 only treatment also indicate a role for O_3 in preferential phenolic degradation during FAC photolysis. Previous work has shown that treatment of DOM by O_3 results in degradation of aromatics within DOM (e.g., ring cleavage of dihydroxybenzenes and phenolic-like compounds) and to decreased DBP formation during subsequent chlorination, highlighting the role of phenolic moieties in DOM as DBP precursors (Gallard and von Gunten 2002, Li et al. 2016). However, it is possible that under the conditions of FAC+light treatment, O_3 levels are low enough relative to DOM concentrations that activated aromatic DBP precursors are *generated* by oxygenation and/or hydroxylation reactions to a greater extent than they are

destroyed (Mao et al. 2014, Riley and Mancy 1978). In this work, HAA and THM formation during FAC+light/FAC only treatment seemed to correlate negatively with conditions favoring higher in situ O_3 levels, supporting the hypothesis that increasing O_3 exposure contributes to the net degradation of organic DBP precursors.

Experiments undertaken here with added radical scavengers indicate that ROS and RHS contribute to both chromophore and fluorophore destruction and non-selective attack and degradation of high molecular weight humic-like substances to form lower molecular weight organic acids. HO^\bullet has been found to react rapidly via hydroxylation of olefins and aromatic compounds and hydrogen abstraction from aliphatic compounds (Dotson et al. 2010, Mvula and von Sonntag 2003, Pan et al. 1993, Varanasi et al. 2018). Cl^\bullet may also react with a variety of aliphatic, aromatic, and olefinic moieties, as well as alcohol groups in DOM via addition, electron-transfer, and/or H-abstraction (Alegre et al. 2000, Martire et al. 2001, Varanasi et al. 2018, Wang et al. 2017). Overall, ROS and/or RHS reactions appear to contribute to the generation of additional DBP precursors. It is hypothesized that HO^\bullet in particular activates aromatic groups by hydroxylation and generates lower MW aldehydes, ketones, and carboxylic acids as transformation products after reacting with higher MW fractions of DOM (Varanasi et al. 2018, Wang et al. 2017). HAA formation increases moderately during FAC only treatment after FAC+light pretreatment when compared to FAC only treatment at equivalent CT_{FAC} , supporting the hypothesis that molecules generated via ROS and RHS reactions with DOM act as HAA precursors (specifically for DCAA and TCAA) during the residual dark chlorination period of FAC+Light/FAC only experiments. Increased THM and HAA formation during FAC+light treatment may also be due to direct attack of DOM by radical species such as HO^\bullet , Cl^\bullet , Br^\bullet , $BrCl^\bullet$, Cl_2^\bullet , or ClO^\bullet – initiating radical chain reactions leading to Cl-addition or C-centered

radical recombination with Cl^\bullet or other halogen radicals (Alegre et al. 2000, Li et al. 2016, Martire et al. 2001, Wang et al. 2015).

One possible explanation for the increases in DBP yields observed during FAC+light treatment, even in the presence of added radical scavengers or under anoxic conditions, is that O_3 and radical species contribute to varying degrees to both degradation and generation of DBP precursors (De Vera et al. 2015, Mao et al. 2014), with precursor generation generally outweighing precursor degradation. Consequently, limiting O_3 formation does not prevent increases in DBP formation due to radical reactions (Li et al. 2016), and limiting HO^\bullet and Cl^\bullet levels does not prevent increases in DBP formation due to $\text{O}(^3\text{P})$ and/or O_3 reactions (Mao et al. 2014, Riley and Mancy 1978).

4. Conclusions

- Application of simulated and natural sunlight-driven FAC photolysis in SRNOM solutions and natural waters resulted in increased yields of regulated organic DBPs (THMs and HAAs), degradation of DOM chromophores and fluorophores, and decreases in average DOM MW due to degradation of higher MW humic substances to lower MW organic acids with minimal mineralization of DOC.
- Subjecting DOM-containing solutions to FAC+light treatment resulted in substantial changes in the ratios of differential absorbances at 280 and 340 nm (corresponding to carboxylic and phenolic DOM moieties), with preferential removal of the 340 nm band, indicating depletion of phenol groups relative to carboxylic groups in the bulk DOM.
- Taken together, these results indicate that FAC+light treatment results in enhanced degradation of UV-absorbing and fluorescent aromatic constituents (phenolic moieties in

particular) of higher MW humic substances by photochemically-generated oxidants including O_3 , HO^\bullet , and possibly Cl^\bullet , ClO^\bullet , Cl_2^\bullet , and $O(^3P)$. Oxidants are expected to participate in aromatic and aliphatic electron transfer, addition, and H-abstraction reactions, in addition to aromatic ring cleavage, resulting in formation of lower MW organic acid byproducts. This process likely results in enhanced formation of DBPs through (a) increased dark halogenation of DBP precursors derived from aromatic ring-cleavage and other DOM degradation pathways; (b) direct halogenation of DBP precursors by RHS such as Cl^\bullet , Br^\bullet , $BrCl^\bullet$, Cl_2^\bullet , or ClO^\bullet ; or (c) a combination of the two. The fact that DBP formation during FAC only treatment subsequent to FAC+light treatment was only moderately higher (for HAAs) than during FAC only treatment suggests that direct halogenation by photochemically-generated RHS may contribute substantially to the enhanced DBP yields observed during sunlight-driven FAC photolysis. It is recommended that future investigations expand on these findings by utilizing model compounds representing various types of DOM constituent groups to evaluate the relative importance of reaction pathways involving ROS, RHS, and O_3 in driving DBP formation during solar FAC photolysis (and UV-driven FAC photolysis in general).

- Application of sunlight-driven FAC photolysis for disinfection is anticipated to lead to increased DBP formation, and will require careful attention to potential impacts on THM and HAA levels. However, because this process can enable inactivation of chlorine resistant pathogens (e.g., *Cryptosporidium* oocysts) at far lower CT_{FAC} values than chlorination alone, the increases in DBP formation inherent to FAC+light treatment may be offset by the ability to operate at significantly decreased CT_{FAC} . In addition, risks of increased DBP formation could be mitigated by limiting applications of sunlight-driven FAC photolysis to short-term

(e.g., emergency) use and/or to appropriate source waters (e.g., those with low DOM and bromide levels, as observed here for treatment of two samples collected from natural surface water sources).

Appendix A. Supplementary data

Supplementary material related to this article can be found at: <http://XXX>

Acknowledgements

This material is based upon work supported by the National Science Foundation under Grant No. CBET-1236303. Additional support from a National Science Foundation Graduate Research Fellowship (ID: 2015177669) for T.R.Y., the National Science Foundation of China (51708279) for W.L., and the University of Washington Mary Gates Research Scholarship for A.G. is gratefully acknowledged. Two anonymous reviewers are thanked for their helpful comments.

References

- Alegre, M.L., Gerones, M., Rosso, J.A., Bertolotti, S.G., Braun, A.M., Martire, D.O. and Gonzalez, M.C. (2000) Kinetic study of the reactions of chlorine atoms and Cl-2(center dot-) radical anions in aqueous solutions. 1. Reaction with benzene. *Journal of Physical Chemistry A* 104(14), 3117-3125.
- Buxton, G.V. and Subhani, M.S. (1972) Radiation-Chemistry and Photochemistry of Oxychlorine Ions .2. Photodecomposition of Aqueous-Solutions of Hypochlorite Ions. *Journal of the Chemical Society-Faraday Transactions I* 68, 958-&.
- Chellam, S. and Krasner, S.W. (2001) Disinfection byproduct relationships and speciation in chlorinated nanofiltered waters. *Environmental Science & Technology* 35(19), 3988-3999.
- Cho, M., Kim, J.H. and Yoon, J. (2006) Investigating synergism during sequential inactivation of *Bacillus subtilis* spores with several disinfectants. *Water Research* 40(15), 2911-2920.
- Cho, M. and Yoon, J. (2007) Quantitative evaluation and application of *Cryptosporidium parvum* inactivation with ozone treatment. *Water Science and Technology* 55(1-2), 241-250.

- Cho, M. and Yoon, J. (2008) Measurement of OH radical CT for inactivating *Cryptosporidium parvum* using photo/ferrioxalate and photo/TiO₂ systems. *Journal of Applied Microbiology* 104(3), 759-766.
- Cory, R.M. and McKnight, D.M. (2005) Fluorescence spectroscopy reveals ubiquitous presence of oxidized and reduced quinones in dissolved organic matter. *Environmental Science & Technology* 39(21), 8142-8149.
- Cowman, G.A. and Singer, P.C. (1996) Effect of bromide ion on haloacetic acid speciation resulting from chlorination and chloramination of aquatic humic substances. *Environmental Science & Technology* 30(1), 16-24.
- De Vera, G.A., Stalter, D., Gernjak, W., Weinberg, H.S., Keller, J. and Farre, M.J. (2015) Towards reducing DBP formation potential of drinking water by favouring direct ozone over hydroxyl radical reactions during ozonation. *Water Research* 87, 49-58.
- Dodd, M.C., Vu, N.V., Le, V.C., Kissner, R., Pham, H.V., Cao, T.H., Berg, M. and Von Gunten, U. (2006) Kinetics and mechanistic aspects of As(III) oxidation by chlorine, chloramines, and ozone: Relevance to drinking water treatment. *Environmental Science and Technology* 40(10), 3285-3292.
- Dotson, A.D., Keen, V.S., Metz, D. and Linden, K.G. (2010) UV/H₂O₂ treatment of drinking water increases post-chlorination DBP formation. *Water Research* 44(12), 3703-3713.
- Dryer, D.J., Korshin, G.V. and Fabbicino, M. (2008) In situ examination of the protonation behavior of fulvic acids using differential absorbance spectroscopy. *Environmental Science & Technology* 42(17), 6644-6649.
- Dulin, D. and Mill, T. (1981) Development and Application of Chemical Actinometers for Solar Irradiance. *Abstracts of Papers of the American Chemical Society* 181(Mar), 82-Envr.
- EPA, U.S. (2005) Technologies and Cost Document for the Final Long Term 2 Enhanced Surface Water Treatment Rule and Final Stage 2 Disinfectants and Disinfection Byproducts Rule. Water, O.o. (ed), National Service Center for Environmental Publications.
- Flury, M. and Papritz, A. (1993) Bromide in the natural environment: Occurrence and Toxicity. *Journal of Environmental Quality* 22, 747-758.
- Forsyth, J.E., Zhou, P.R., Mao, Q.X., Asato, S.S., Meschke, J.S. and Dodd, M.C. (2013) Enhanced Inactivation of *Bacillus subtilis* Spores during Solar Photolysis of Free Available Chlorine. *Environmental Science & Technology* 47(22), 12976-12984.
- Gallard, H. and von Gunten, U. (2002) Chlorination of natural organic matter: kinetics of chlorination and of THM formation. *Water Research* 36(1), 65-74.
- Gao, Y. and Korshin, G. (2013) Effects of NOM properties on copper release from model solid phases. *Water Research* 47(14), 4843-4852.
- Her, N., Amy, G., McKnight, D., Sohn, J. and Yoon, Y.M. (2003) Characterization of DOM as a function of MW by fluorescence EEM and HPLC-SEC using UVA, DOC, and fluorescence detection. *Water Research* 37(17), 4295-4303.
- Hua, B., Veum, K., Yang, J., Jones, J. and Deng, B.L. (2010) Parallel factor analysis of fluorescence EEM spectra to identify THM precursors in lake waters. *Environmental Monitoring and Assessment* 161(1-4), 71-81.
- Hua, G.H. and Reckhow, D.A. (2013) Effect of pre-ozonation on the formation and speciation of DBPs. *Water Research* 47(13), 4322-4330.

- Huber, S.A., Balz, A., Abert, M. and Pronk, W. (2011) Characterisation of aquatic humic and non-humic matter with size-exclusion chromatography - organic carbon detection - organic nitrogen detection (LC-OCD-OND). *Water Research* 45(2), 879-885.
- Ishii, S.K.L. and Boyer, T.H. (2012) Behavior of Reoccurring PARAFAC Components in Fluorescent Dissolved Organic Matter in Natural and Engineered Systems: A Critical Review. *Environmental Science & Technology* 46(4), 2006-2017.
- Korshin, G.V., Kumke, M.U., Li, C.W. and Frimmel, F.H. (1999) Influence of chlorination on chromophores and fluorophores in humic substances. *Environmental Science & Technology* 33(8), 1207-1212.
- Korshin, G.V., Li, C.W. and Benjamin, M.M. (1997) The decrease of UV absorbance as an indicator of TOX formation. *Water Research* 31(4), 946-949.
- Korshin, G.V., Wu, W.W., Benjamin, M.M. and Hemingway, O. (2002) Correlations between differential absorbance and the formation of individual DBPs. *Water Research* 36(13), 3273-3282.
- Laszakovits, J.R., Berg, S.M., Anderson, B.G., O'Brien, J.E., Wammer, K.H. and Sharpless, C.M. (2017) p-Nitroanisole/Pyridine and p-Nitroacetophenone/Pyridine Actinometers Revisited: Quantum Yield in Comparison to Ferrioxalate. *Environmental Science & Technology Letters* 4(1), 11-14.
- Li, T., Jiang, Y., An, X.Q., Liu, H.J., Hu, C. and Qu, J.H. (2016) Transformation of humic acid and halogenated byproduct formation in UV-chlorine processes. *Water Research* 102, 421-427.
- Liang, L. and Singer, P.C. (2003) Factors influencing the formation and relative distribution of haloacetic acids and trihalomethanes in drinking water. *Environmental Science & Technology* 37(13), 2920-2928.
- Liu, W., Zhang, Z., Yang, X., Xu, Y. and Liang, Y. (2012) Effects of UV irradiation and UV/chlorine co-exposure on natural organic matter in water. *Science of the Total Environment* 414, 576-584.
- Lv, X.T., Zhang, X., Du, Y., Wu, Q.Y., Lu, Y. and Hu, H.Y. (2017) Solar light irradiation significantly reduced cytotoxicity and disinfection byproducts in chlorinated reclaimed water. *Water Research* 125, 162-169.
- Mao, Y.Q., Wang, X.M., Yang, H.W., Wang, H.Y. and Xie, Y.F.F. (2014) Effects of ozonation on disinfection byproduct formation and speciation during subsequent chlorination. *Chemosphere* 117, 515-520.
- Martire, D.O., Rosso, J.A., Bertolotti, S., Le Roux, G.C., Braun, A.M. and Gonzalez, M.C. (2001) Kinetic study of the reactions of chlorine atoms and Cl(2)(center dot)-radical anions in aqueous solutions. II. Toluene, benzoic acid, and chlorobenzene. *Journal of Physical Chemistry A* 105(22), 5385-5392.
- McGuigan, K.G., Conroy, R.M., Mosler, H.J., du Preez, M., Ubomba-Jaswa, E. and Fernandez-Ibanez, P. (2012) Solar Water Disinfection (SODIS): A review from bench-top to roof-top. *Journal of Hazardous Materials* 7(53), 29-46.
- Medema, G.T., P., Blokker, M.; Deere, D.; Davidson, A.; Charles, P.; and Loret, J.F. (2009) Risk Assessment of Cryptosporidium in Drinking Water. *Public Health and Environment: Water, S., Hygiene and Health* (ed), WHO Press, Geneva, Switzerland.
- Munch, D.J.M., J.W.; and Pawlecki, A.M. (1995) Method 552.2, Determination of Haloacetic acids and Dalapon in Drinking Water by Liquid-Liquid Extraction, Derivatization and

- Gas Chromatography with Electron Capture Detection. Laboratory, N.E.R. (ed), Cincinnati, OH.
- Mvula, E. and von Sonntag, C. (2003) Ozonolysis of phenols in aqueous solution. *Organic & Biomolecular Chemistry* 1(10), 1749-1756.
- Nowell, L.H. and Hoigne, J. (1992a) Photolysis of Aqueous Chlorine at Sunlight and Ultraviolet Wavelengths .1. Degradation Rates. *Water Research* 26(5), 593-598.
- Nowell, L.H. and Hoigne, J. (1992b) Photolysis of Aqueous Chlorine at Sunlight and Ultraviolet Wavelengths .2. Hydroxyl Radical Production. *Water Research* 26(5), 599-605.
- Oliver, B.G. and Carey, J.H. (1977) Photochemical Production of Chlorinated Organics in Aqueous-Solutions Containing Chlorine. *Environmental Science & Technology* 11(9), 893-895.
- Painter, J.E., Hlavsa, M.C., Collier, S.A., Xiao, L.H. and Yoder, J.S. (2015) Cryptosporidiosis Surveillance - United States, 2011-2012. *Mmwr Surveillance Summaries* 64(3), 1-13.
- Pan, X.M., Schuchmann, M.N. and Vonsonntag, C. (1993) Oxidation of Benzene by the Oh Radical - a Product and Pulse-Radiolysis Study in Oxygenated Aqueous-Solution. *Journal of the Chemical Society-Perkin Transactions 2* (3), 289-297.
- Pisarenko, A.N., Stanford, B.D., Snyder, S.A., Rivera, S.B. and Boal, A.K. (2013) Investigation of the use of Chlorine Based Advanced Oxidation in Surface Water: Oxidation of Natural Organic Matter and Formation of Disinfection Byproducts. *Journal of Advanced Oxidation Technologies* 16(1), 137-150.
- Remucal, C.K. and Manley, D. (2016) Emerging investigators series: the efficacy of chlorine photolysis as an advanced oxidation process for drinking water treatment. *Environmental Science-Water Research & Technology* 2(4), 565-579.
- Riley, T.L. and Mancy, K.H. (1978) The effect of preozonation on chloroform production in the chlorine disinfection processes, Ann Arbor Science, Ann Arbor, MI.
- Rook, J.J. (1977) Chlorination Reactions of Fulvic Acids in Natural-Waters. *Environmental Science & Technology* 11(5), 478-482.
- Sharpless, C.M. and Blough, N.V. (2014) The importance of charge-transfer interactions in determining chromophoric dissolved organic matter (CDOM) optical and photochemical properties. *Environmental Science-Processes & Impacts* 16(4), 654-671.
- Shu, Z.Q., Li, C., Belosevic, M., Bolton, J.R. and El-Din, M.G. (2014) Application of a Solar UV/Chlorine Advanced Oxidation Process to Oil Sands Process-Affected Water Remediation. *Environmental Science & Technology* 48(16), 9692-9701.
- Simard, S., Tardif, R. and Rodriguez, M.J. (2013) Variability of chlorination by-product occurrence in water of indoor and outdoor swimming pools. *Water Research* 47(5), 1763-1772.
- Soltermann, F., Abegglen, C., Gotz, C. and Von Gunten, U. (2016) Bromide sources and loads in Swiss surface waters and their relevance for bromate formation during wastewater ozonation. *Environmental Science & Technology* 50, 9825-9834.
- Varanasi, L., Coscarelli, E., Khaksari, M., Mazzoleni, L.R. and Minakata, D. (2018) Transformations of dissolved organic matter induced by UV photolysis, hydroxyl radicals, chlorine radicals, and sulfate radicals in aqueous-phase UV-based advanced oxidation processes. *Water Research* 135, 22-30.
- Wang, D., Bolton, J.R., Andrews, S.A. and Hofmann, R. (2015) Formation of disinfection by-products in the ultraviolet/chlorine advanced oxidation process. *Science of the Total Environment* 518, 49-57.

- Wang, W.L., Zhang, X., Wu, Q.Y., Du, Y. and Hu, H.Y. (2017) Degradation of natural organic matter by UV/chlorine oxidation: Molecular decomposition, formation of oxidation byproducts and cytotoxicity. *Water Research* 124, 251-258.
- WHO (2017) Guidelines for drinking-water quality: fourth edition incorporating the first addendum, World Health Organization (WHO), Geneva.
- Xiang, Y., Fang, J. and Shang, C. (2016) Kinetics and pathways of ibuprofen degradation by the UV/Chlorine advanced oxidation. *Water Research* 90, 301-308.
- Yang, X., Sun, J., Fu, W., Shang, C., Li, Y., Chen, Y., Gan, W. and Fang, J. (2016) PPCP degradation by UV/chlorine treatment and its impact on DBP formation potential in real waters. *Water Research* 98, 309-318.
- Zhou, P., Di Giovanni, G.D., Meschke, J.S. and Dodd, M.C. (2014) Enhanced Inactivation of *Cryptosporidium parvum* Oocysts during Solar Photolysis of Free Available Chlorine. *Environmental Science & Technology Letters* 1(11), 453-458.

Table and Figure Captions

Table 1. Summary of chlorine photolysis reactions and quantum yields

		$\Phi(254\text{ nm})$	$\Phi(313\text{ nm})$	$\Phi(365\text{ nm})$
$\text{HOCl} + h\nu \rightarrow \text{HO}^\bullet + \text{Cl}^\bullet$	(1a)	0.46-1.4 ^{a-c}	1 ^{d*}	N/A
$\text{OCl}^- + h\nu \rightarrow \text{O}^\bullet + \text{Cl}^\bullet$	(1b)	0.278 ^e	0.127 ^e	0.08 ^e
$\text{OCl}^- + h\nu \rightarrow \text{O}(^3\text{P}) + \text{Cl}^-$	(2)	0.074 ^e	0.075 ^e	0.28 ^e

^a(Watts et al 2007), ^b(Jin et al 2011), ^c(Wang et al 2012), ^{*}at approximately 310 nm ^d(Molina et al 1980), ^e(Buxton and Subhani 1972), N/A = not available

Figure 1. (a) HAA5; and (c) TTHM formation in pH 8 (10 mM) phosphate buffer with 2 mg/L SRNOM comparing FAC only treatment (0 minutes in the solar simulator) with FAC+light/FAC only treatment at varying bromide concentration (0-200 $\mu\text{g/L}$) and temperature (10°C or 25°C); and (b) HAA5; and (d) TTHM formation in pH 6 (10 mM) phosphate buffer with 2 mg/L SRNOM at 10 °C comparing FAC only treatment with FAC+light/FAC only treatment at varying bromide concentration (0-200 $\mu\text{g/L}$). All samples utilized $[\text{FAC}]_0 \sim 8\text{ mg/L}$ as Cl_2 and targeted $CT_{\text{FAC}} = 400\text{ (mg/L)} \times \text{min}$.

Figure 2. (a) HAA5 and (b) TTHM formation with saturated (1.6mM) dissolved O_2 (black), 50 mM HCO_3^- (red), 50 mM $t\text{-BuOH}$ (green), initially anoxic conditions (yellow), or no alteration (blue) after exposure to FAC only or varied FAC+light/FAC only treatment. All solutions were prepared in 10 mM phosphate buffer at pH 8 at 10 °C with 2 mg/L SRNOM, 200 $\mu\text{g/L}$ bromide, and $[\text{FAC}]_0 \sim 8\text{ mg/L}$ as Cl_2 , and targeted $CT_{\text{FAC}} = 400\text{ (mg/L)} \times \text{min}$.

Figure 3. Comparison of TTHM and HAA5 formation during FAC only, FAC+light, and FAC+light/FAC only treatment targeting $CT_{\text{FAC}} = 400\text{ (mg/L)} \times \text{min}$ at 10 °C for (a) pH 8; and (b) pH 6. All samples were prepared in 10 mM phosphate buffer with 2 mg/L SRNOM, 200 $\mu\text{g/L}$ bromide, and $[\text{FAC}]_0 \sim 8\text{ mg/L}$ as Cl_2 .

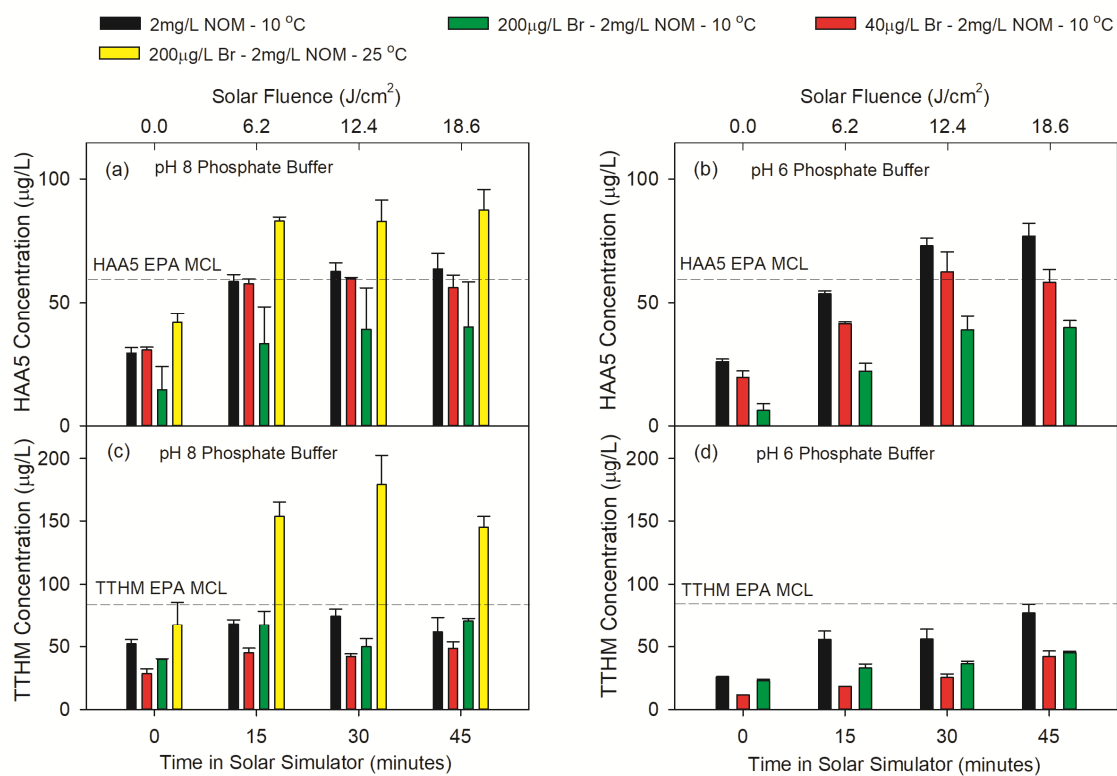
Figure 4. (a) HAA5; and (b) TTHM formation in natural waters during FAC only, Light only/FAC only, and FAC+light/FAC only treatment. For all samples the temperature was 10 °C, $[\text{FAC}]_0 \sim 8\text{ mg/L}$ as Cl_2 , and $CT_{\text{FAC}} = 400\text{ (mg/L)} \times \text{min}$. Local Reservoir – pH = 8.05, 0.5 mg/L as C with 24.5 $\mu\text{g/L}$ bromide and 30.7 mg/L as CaCO_3 alkalinity. Lake Washington – pH = 8.10, 2.4 mg/L as C with 23.7 $\mu\text{g/L}$ bromide and 38.0 mg/L as CaCO_3 alkalinity. Samples labeled “+ Br” included an additional 200 $\mu\text{g/L}$ of bromide in excess of natural levels.

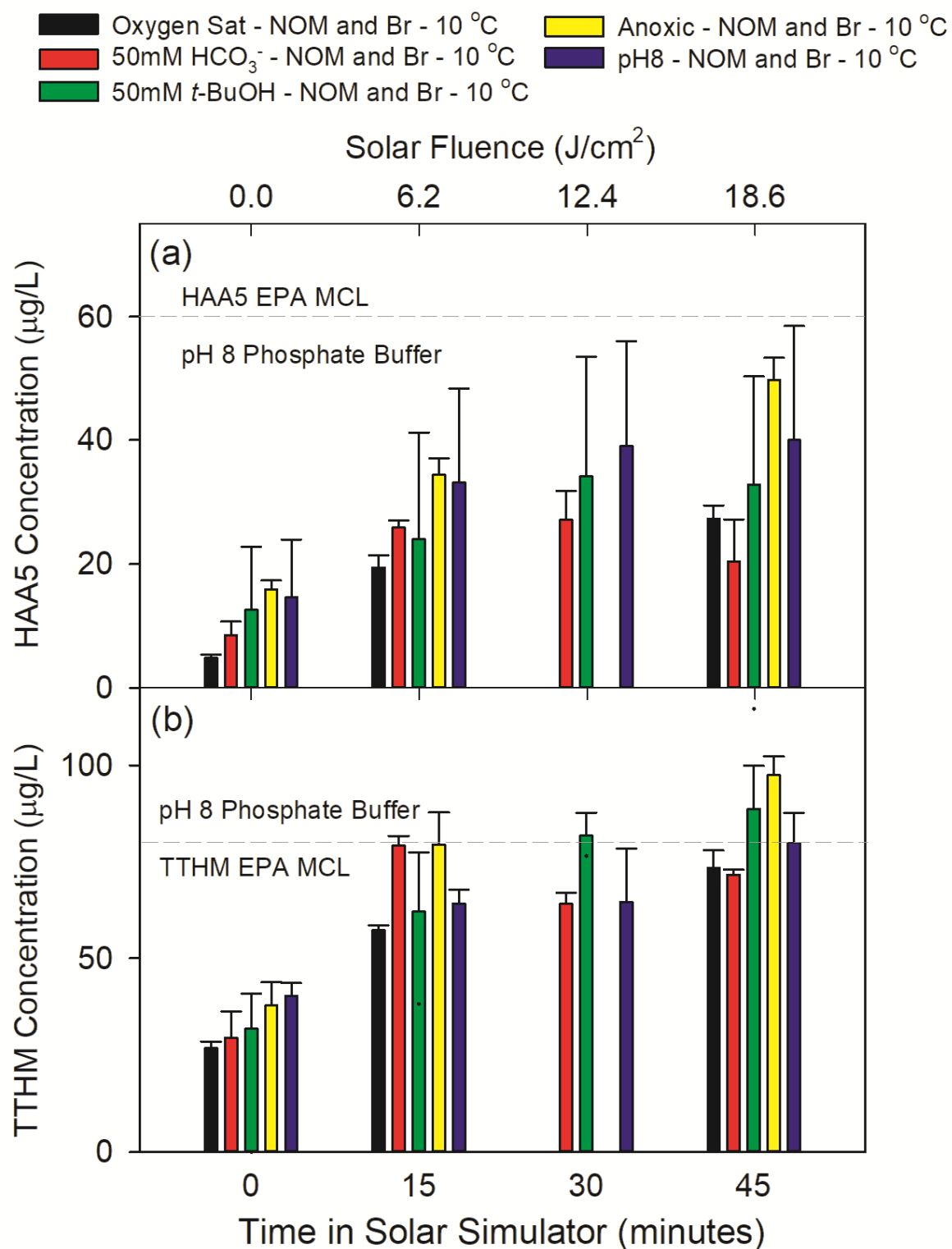
733

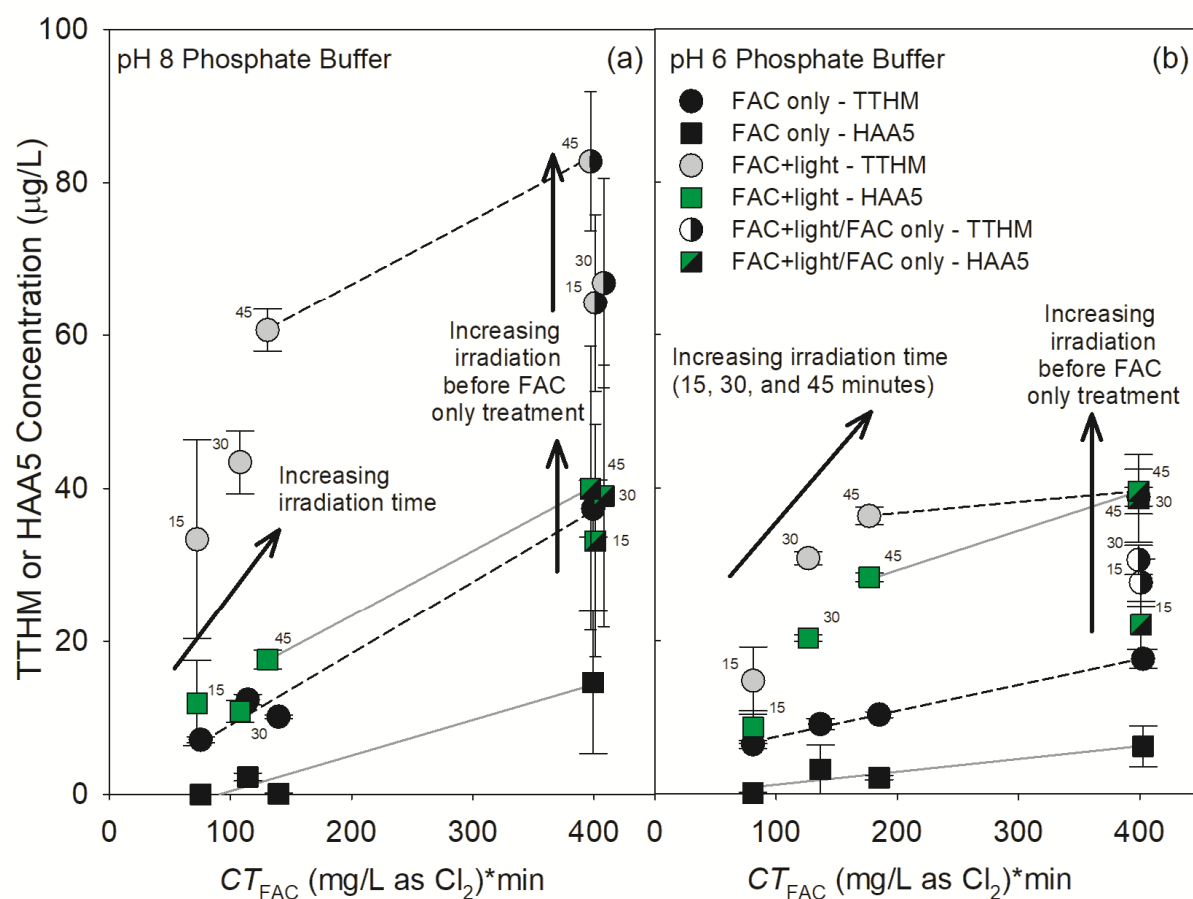
734 **Figure 5.** (a) Bulk UV absorbance at 254 nm (white squares) and fluorescence (filled circles).
 735 (b)-(d) SEC data for (b) DOC, (c) UV absorbance at 254 nm, and (d) fluorescence (Ex: 320 nm,
 736 Em: 450 nm), summarizing total chromatographic peak areas normalized by untreated samples
 737 (white circles), and MW estimated from signal intensity-weighted retention times (green
 738 triangles; Text S7 for details). Data is from experiments with pH 8, 10mM phosphate buffered
 739 solutions containing 2 mg/L SRNOM and 200 $\mu\text{g/L Br}^-$ at 10 °C, after Light only, FAC only,
 740 Light only(45 min. irr.)/FAC only, FAC+Light, and FAC+Light(45 min. irr.)/FAC only
 741 treatment (x-axis represents treatment conditions, not time series). FAC only, Light only/FAC
 742 only, and FAC+light/FAC only experiments targeted $CT_{\text{FAC}} = 400 \text{ (mg/L)} \times \text{min}$.

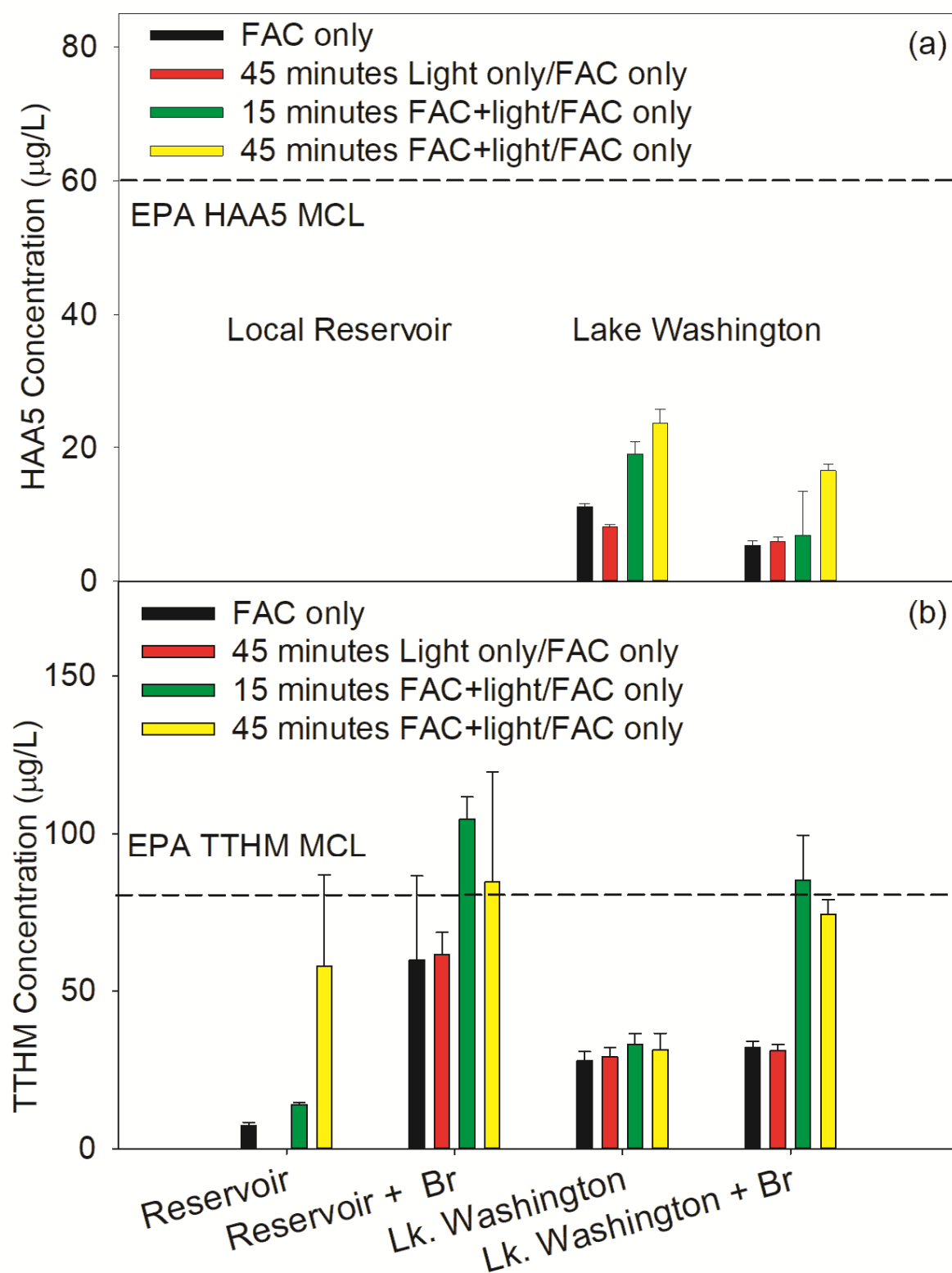
743

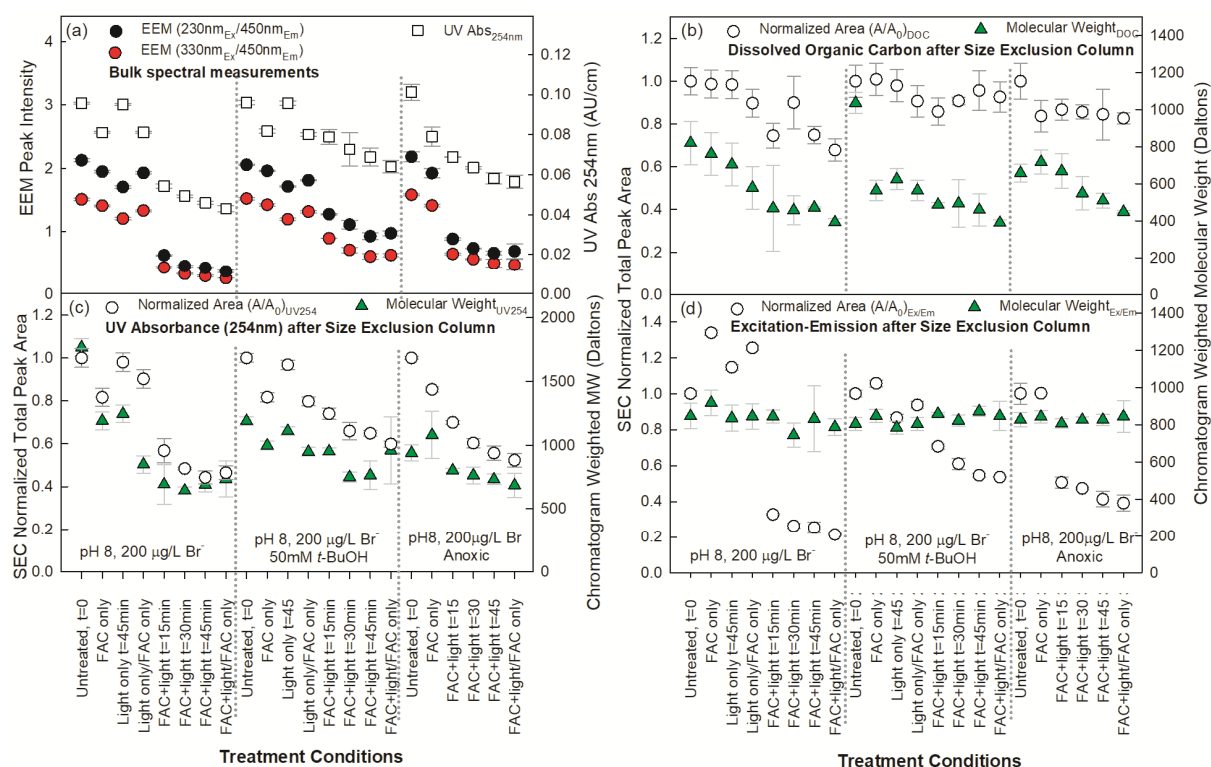
744 **Figure 6.** Sample DAS spectra for 2 mg/L SRNOM in 0.5 mM phosphate buffer subjected to (a)
 745 no treatment; (b) FAC only treatment at pH 8 to $CT_{\text{FAC}} = 160 \text{ (mg/L)} \times \text{min}$; (c) FAC+light
 746 treatment at pH 8 to $CT_{\text{FAC}} = 160 \text{ (mg/L)} \times \text{min}$; (d) FAC+light treatment at pH 8 with initially
 747 anoxic conditions, $CT_{\text{FAC}} = 77 \text{ (mg/L)} \times \text{min}$; (e) FAC+light treatment at pH 8 with 50mM *tert*-
 748 butanol to $CT_{\text{FAC}} = 160 \text{ (mg/L)} \times \text{min}$; and (f) O_3 only treatment at pH 8. All solutions prepared in
 749 of 0.5 mM phosphate buffer at 25 °C with 2 mg/L SRNOM and $[\text{FAC}]_0 \sim 8 \text{ mg/L}$ as Cl_2 .

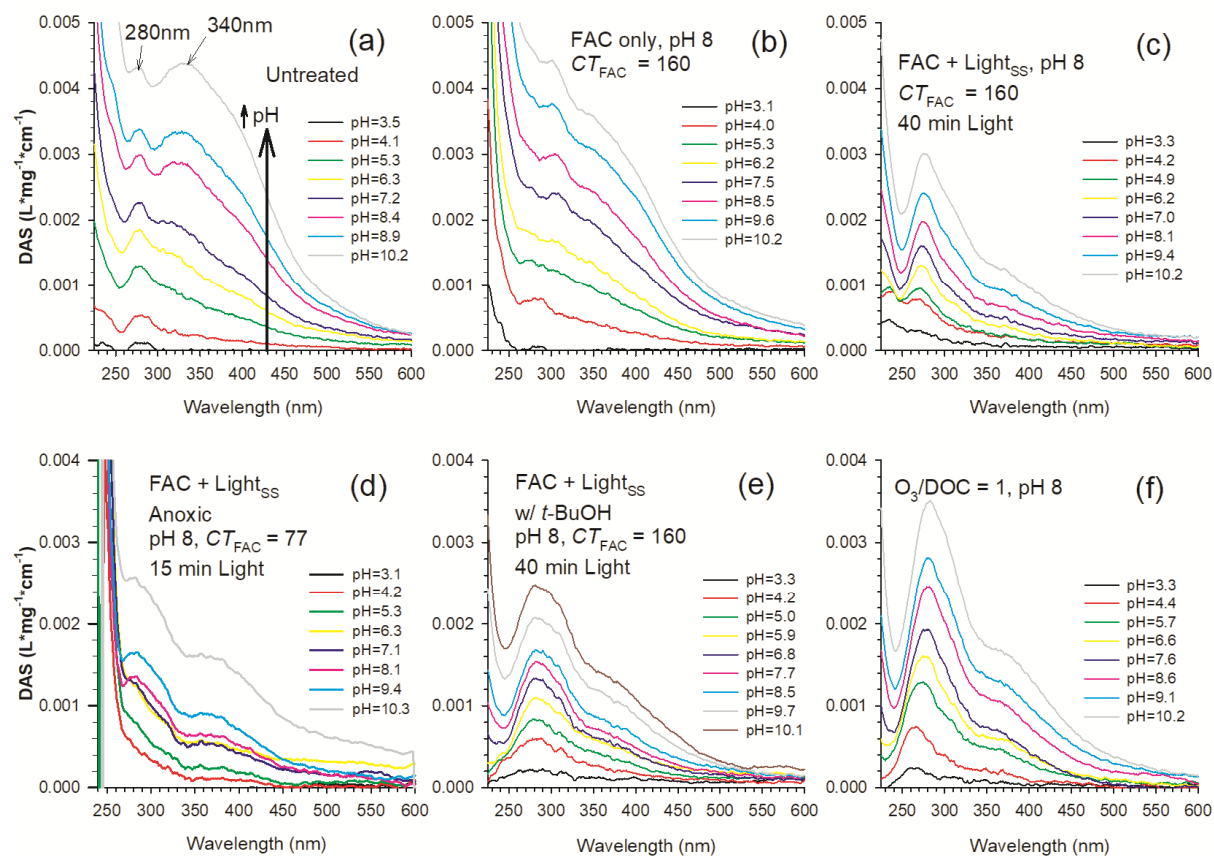












- Solar chlorine photolysis increases THM and HAA formation in DOM-containing waters
- DBP formation correlates with extensive photobleaching and decreased MW of DOM
- Photogenerated ROS, RHS, and O₃ drive DBP precursor generation and destruction
- THM and HAA levels can be maintained below MCLs in waters with low DOM and bromide
- Use of solar chlorine photolysis for disinfection requires attention to DBP impacts